Liquid Crystals
Publication details, including instructions for authors and subscription information:
http://www.informaworld.com/smpp/title~content=t713926090

Approximate analytic solutions for the director profile of homogeneously aligned nematic liquid crystals

I. Abdulhalim[a]; D. Menashe[b]
[a] Department of Electrooptic Engineering, Ben Gurion University, Beer Sheva, Israel [b] RED-C Optical Networks Ltd, Tel-Aviv, Israel

Online publication date: 11 February 2010

To cite this Article Abdulhalim, I. and Menashe, D.(2010) 'Approximate analytic solutions for the director profile of homogeneously aligned nematic liquid crystals', Liquid Crystals, 37: 2, 233 — 239
To link to this Article: DOI: 10.1080/02678290903506024
URL: http://dx.doi.org/10.1080/02678290903506024

Liquid Crystals,
Vol. 37, No. 2, February 2010, 233–239

Taylor & Francis
Taylor & Francis Group

Approximate analytic solutions for the director profile of homogeneously aligned nematic liquid crystals

I. Abdulhalim[a]* and D. Menashe[b]

[a]*Department of Electrooptic Engineering, Ben Gurion University, Beer Sheva, Israel;* [b]*RED-C Optical Networks Ltd, Atidim Tech. Park, Tel-Aviv 61580, Israel*

(Received 20 May 2009; final version received 23 November 2009)

Simple analytic solutions to the equations governing the nematic liquid crystal director profiles under an external voltage and arbitrary anchoring energy, taking into consideration the non-uniform field distribution, are presented. Exact numerical results are compared to the analytic solutions showing good agreement particularly for the case of strong anchoring. The usefulness of the approximate analytic solutions is remarkable for the quick design of liquid crystal devices and understanding the dependence of the optical response on voltage and material parameters.

1. Introduction

The interest in liquid crystal (LC) devices based on the homogeneously aligned nematic LCs (HANLCs) has grown recently due to their importance not only for displays but also for a variety of other applications. As tunable birefringent plates they have been used to build modulators, tunable filters, shutters, variable retarders and polarisation controllers [1]. The response of HANLCs to an external electric field is crucial for the design of these devices due to the fact that the molecules near the boundaries respond differently from those in the centre of the cell. This fact is expressed by the anchoring strength of the boundaries determined by the surface treatment such as the alignment layers used, the rubbing or ultraviolet (UV) irradiation conditions used, the LC material and the substrates [2,3]. The anchoring strength is expressed by the anchoring energy, which does not have a well-determined form. However, a generalised form was proposed recently [4] which is also able to consider asymmetric boundary conditions based on the Rapini–Papoular [5] anchoring energy form. The exact simulation of the director profiles has been carried out numerically by several investigators [6] with several improvements to the calculation algorithm [7,8]. Approximate analytic solutions exist for special cases either for the small-angle approximation or in the form of Jacobian-elliptic functions when an isotropic elastic constant is assumed [9,10]. In both cases the non-uniformity of the electric field inside the LC device is not considered and fixed boundary orientations are assumed. When the anchoring energy is finite, the boundary conditions become variable with the field and for this case no approximate analytic solutions exist. In this article we present an approximate analytic solution for the general case, comparing it with the exact numerical solutions and showing that it is a good approximation that is adequate for the design of the optical response of LC devices.

2. Formulations

The free energy per unit area of the LC cell consists of three parts:

$$F = F_{\text{elastic}} + F_{\text{EM}} + F_{\text{boundary}}. \tag{1}$$

F_{elastic} is the elastic free energy given by

$$F_{\text{elastic}} = \int_0^d \frac{1}{2}\left(K_{11}\cos^2\theta + K_{33}\sin^2\theta\right)\left(\frac{d\theta}{dz}\right)^2 dz, \tag{2}$$

where d is the cell thickness, z is the coordinate along the cell normal, K_{11} is the splay elastic constant and K_{33} is the bend elastic constant.

F_{EM} is the electromagnetic free energy given by

$$F_{\text{EM}} = -\frac{1}{2}V_{\text{Ext}}^2 C_{\text{Tot}}, \tag{3}$$

where V_{Ext} is the external voltage (over the entire device) and C_{Tot} is the total capacitance of the device per unit area given by

$$\frac{1}{C_{\text{Tot}}} = \frac{1}{C_{\text{Diel}}} + \frac{1}{C_{\text{LC}}}. \tag{4}$$

*Corresponding author. Email: abdulhlm@bgu.ac.il

ISSN 0267-8292 print/ISSN 1366-5855 online

DOI: 10.1080/02678290903506024
http://www.informaworld.com

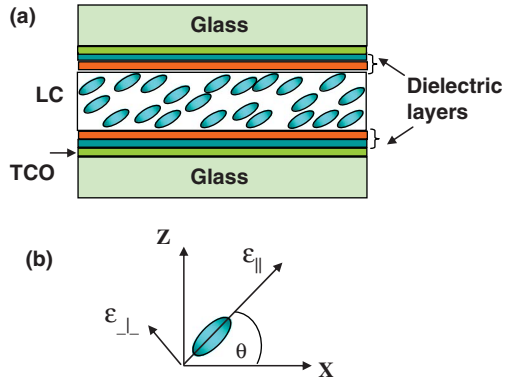

Figure 1. (a) Schematic diagram of a general homogeneously aligned nematic LC device. (b) Geometry of the LC molecular orientation.

Here C_{Diel} is the total capacitance per unit area of all the dielectric layers apart from the LC such as the alignment and passivation layers (Figure 1) and C_{LC} is the capacitance per unit area of the LC cell given by

$$C_{\mathrm{LC}} = \varepsilon_0 \varepsilon_\perp \Big/ \int_0^d \frac{dz}{1+\gamma \sin^2\theta} \tag{5}$$

with

$$\gamma = \frac{\Delta\varepsilon}{\varepsilon_\perp} = \frac{\varepsilon_{||} - \varepsilon_\perp}{\varepsilon_\perp}. \tag{6}$$

F_{boundary} is the boundary free energy given by

$$F_{\mathrm{boundary}} = \frac{1}{2} W_1 \sin^2(\theta(0)-\theta_1)\left[1+\xi \sin^2(\theta(0)-\theta_1)\right] + \frac{1}{2} W_2 \sin^2(\theta(d)-\theta_2)\left[1+\xi \sin^2(\theta(d)-\theta_2)\right] \tag{7}$$

where $W_{1,2}$ is the anchoring energy per unit area at the z = 0,d boundaries respectively, $\theta_{1,2}$ are the pretilt angles at these boundaries and ξ is a constant [4].

It is important to note that both the anchoring energy and the pretilt enter into the model as independent parameters. Practically speaking, there is probably strong correlation between these two parameters, in the sense that a polyimide that exhibits pretilt is more likely to have weak anchoring energy. However, these parameters are often measured independently of each other [11–13], and it appears that they can behave independently as well [13,14]. In particular, the latter reference shows how the anchoring energy can be changed by irradiation with depolarised light, without changing the pretilt.

Using the calculus of variations [15] it is possible to derive from the free energy three equations governing the steady-state director distribution: one for the bulk $0 < z < d$,

$$\left(K_{11}\cos^2\theta + K_{33}\sin^2\theta\right)\frac{d^2\theta}{dz^2} + \left(K_{33}-K_{11}\right)\sin\theta\cos\theta\left(\frac{d\theta}{dz}\right)^2 + V_{\mathrm{Ext}}^2 \frac{C_{\mathrm{Tot}}^2}{\varepsilon_0\varepsilon_\perp}\frac{\gamma\sin\theta\cos\theta}{\left(1+\gamma\sin^2\theta\right)^2} = 0, \tag{8}$$

and one for each of the boundaries $z = 0$,

$$\left(K_{11}\cos^2\theta(0) + K_{33}\sin^2\theta(0)\right)\left.\frac{d\theta}{dz}\right|_{Z=0} = W_1 \sin(\theta(0)-\theta_1)\cos(\theta(0)-\theta_1)\left[1+2\xi\sin^2(\theta(0)-\theta_1)\right] \tag{9}$$

and $z = d$,

$$\left(K_{11}\cos^2\theta(d) + K_{33}\sin^2\theta(d)\right)\left.\frac{d\theta}{dz}\right|_{Z=d} = -W_2 \sin(\theta(d)-\theta_2)\cos(\theta(d)-\theta_2)\left[1+2\xi\sin^2(\theta(d)-\theta_2)\right]. \tag{10}$$

The derivation of these equations is straightforward although the fact that F_{EM} is not a linear function of an integral forms some complication. The solution of Equation (8) together with the boundary conditions (9) and (10) yield the LC director profile; however, the capacitance C_{Tot} depends on the profile through Equation (4), so all the equations must be solved self-consistently.

3. Numerical routine

Equations (5) and (8)–(10) may be written in the following dimensionless forms:

$$\frac{d^2\theta}{dz_r^2} = -\frac{1}{2}\left[\kappa\left(\frac{d\theta}{dz_r}\right)^2 + \left(\frac{\pi V_r}{(I+C_r)\left(1+\gamma\sin^2\theta\right)}\right)^2\right]\frac{\sin(2\theta)}{\left(1+\kappa\sin^2\theta\right)}, \tag{11}$$

$$\left(1+\kappa\sin^2\theta(0)\right)\left.\frac{d\theta}{dz_r}\right|_{Z_r=0} = W_{1,r}\sin(\theta(0)-\theta_1)\cos(\theta(0)-\theta_1)\left[1+2\xi\sin^2(\theta(0)-\theta_1)\right], \tag{12}$$

$$\left(1+\kappa\sin^2\theta(1)\right)\left.\frac{d\theta}{dz_r}\right|_{Z_r=1} = -W_{2,r}\sin(\theta(1)-\theta_2)\cos(\theta(1)-\theta_2)\left[1+2\xi\sin^2(\theta(1)-\theta_2)\right], \quad (13)$$

$$I=\int_0^1 \frac{dz_r}{1+\gamma\sin^2\theta}, \quad (14)$$

where γ is given by (6), and

- $z_r \equiv z/d$ is the normalised coordinate;
- $\kappa \equiv \frac{K_{33}-K_{11}}{K_{11}}$;
- $V_r = V_{\mathrm{Ext}}/V_{\mathrm{thf}}$ is the voltage normalised to the Frederick's threshold voltage $V_{\mathrm{thf}} \equiv \pi\sqrt{\frac{K_{11}}{\varepsilon_0\Delta\varepsilon}}$;
- $C_r \equiv \frac{\varepsilon_0\varepsilon_\perp}{dC_{\mathrm{Diel}}}$ is the LC capacitance per unit area at zero voltage normalised to the dielectric capacitance per unit area;
- $W_{i,r} \equiv \frac{W_i d}{K_{11}}$ is the normalised anchoring strength with $i = 1,2$.

Equation (11) together with the boundary conditions (12) and (13) are solved using the matlab solver 'BVP4C'. Initially, I is set to unity and the equation is solved. Then I is calculated according to the profile and the equation is solved again with the new value of I. This process continues until the solution converges. It was found that ten iterations are sufficient to achieve convergence. Note the following points regarding the routine.

- In order to use the 'BVP4C' solver it is necessary to transform Equation (11) from a second-order differential equation to two first-order equations in the standard manner.
- The initial guess for the 'BVP4C' solver is taken as $\theta(z_r) \equiv \pi/2$, $\theta'(z_r) \equiv 0$.
- For the initial iteration we set $\gamma = 1$ and use fixed boundary conditions, i.e. $\theta(0) = \theta_1$ and $\theta(1) = \theta_2$. This is necessary to achieve an initial stable solution. For the following iterations the correct value of γ and correct boundary conditions are used.
- For small values of the normalised anchoring energy $W_{i,r} < 20$ the solution can become unstable at high voltages. To avoid this we initially begin with a large value $W_{i,r} = 1250$ and gradually decrease it until we reach the correct value. This is done as part of the ten iterations used to reach a solution.

4. Approximate analytic solutions

By minimising the free energy on the surfaces the following expression is found for the boundary tilt angle versus voltage:

$$\theta(z_r=0,1) \approx \theta_{1,2} + \arcsin\left(\sqrt{\frac{-b+\sqrt{b^2-4ac_{1,2}}}{2a}}\right), \quad (15)$$

where $\theta_{1,2}$ are the pretilt angles at the two surfaces (at zero voltage) and

$$a = (1+2\xi)(\gamma+2\kappa+\gamma\kappa+2\xi(\gamma+\gamma\kappa-2)),$$

$$b = (1+2\xi)^2(\kappa+1),$$

$$c = -V_r^2\lambda_{r1,2}^2(1+\kappa)^3,$$

with $\lambda_{r1,2} = \frac{\pi}{W_{r1,2}}$ being the anchoring extrapolation length normalised to the cell thickness. Note that when the boundaries are asymmetric the steady-state tilt angles at the two boundaries are different. Our interest is in the cases of symmetric boundary conditions, that is, $W_{1,2} = W$, $\lambda_{r1,2} = \lambda_r$, $\theta_{1,2} = \theta_0$, $\theta(z_r=0) = \theta(z_r=1) = \theta_b$. In this case, Equation (15) is written as

$$\theta_b(V_r) \approx \theta_0 + \arcsin\left(\sqrt{\frac{-b+\sqrt{b^2-4ac}}{2a}}\right). \quad (16)$$

Note that for strong anchoring, $\lambda_r \to 0$, the tilt angle at the boundary is fixed to the pretilt value. Hence for the case of strong anchoring the behaviour of the tilt angle profile is universal and does not depend on the anchoring strength because the only parameter that contains the thickness d not normalised is λ_r. On the other hand, when the anchoring is finite there is some dependence on the thickness through the parameter λ_r. In this case, instead of the voltage dependence of the switching, an electric field E dependence starts to appear as can be seen from the expression for the parameter c,

$$c = -V_r^2\lambda_{r1,2}^2(1+\kappa)^3 = -E^2\varepsilon_0\Delta\varepsilon(1+\kappa)^3/W^2.$$

For small angles, the profile is usually approximated with the form

$$\theta(z) \approx \theta_b + \theta_m\sin(\pi z_r), \quad (17)$$

where θ_m is the angle in the middle of the cell. This approximation is valid only for very small angles ($\theta_m \approx 5 - 10^{\circ}$). In order to find better approximations we relied on the fact that nonlinear differential equations with close similarity to Equation (11) exhibit kink-type solutions [16–18] containing the functions arctan(x) and arctan(exp(x)) where $x = z_r/\chi_r$ for the kink with origin at $z_r = 0$, while $x = (1 - z_r)/\chi_r$ for the kink starting at $z_r = 1$. Here $\chi_r = C/(\pi V_r)$ with $C = 1 + \lambda_r$, so that for the case of infinite anchoring $\lambda_r = 0$ and $C = 1$. The solution is therefore a combination of two such kinks and it has to satisfy the boundary conditions and the fact that the tilt angle in the centre of the cell is θ_m. For the case of small angles up to $\theta_m \approx 30^{\circ}$ we found the following analytic expression:

$$\theta(z_r) \approx \theta_b(V_r) + (\theta_m(V_r) - \theta_b(V_r)) \left[\frac{\arctan(\exp(z_r/\chi_r)) + \arctan(\exp((1 - z_r)/\chi_r)) - \arctan(\exp(1/\chi_r)) - \pi/4}{2\arctan(\exp(0.5/\chi_r)) - \arctan(\exp(1/\chi_r)) - \pi/4}\right]. \quad (18)$$

This approximation was found to give agreement with the exact profile up to better than fractions of a degree for the case of fixed boundaries. For angles $\theta_m > 30^{\circ}$ a better approximation is the following:

$$\theta(z_r) \approx \theta_b(V_r) + (\theta_m(V_r) - \theta_b(V_r)) \left[\frac{\arctan(z_r/\chi_r) + \arctan((1 - z_r)/\chi_r) - \arctan(1/\chi_r)}{2\arctan(0.5/\chi_r) - \arctan(1/\chi_r)}\right]. \quad (19)$$

The approximate expression given in Equation (19) gives very satisfactory agreement with the exact profile over the entire range of tilt angles. Another possibility is to take the average between the two expressions of Equations (18) and (19). Note that the parameter $\chi_r = C/(\pi V_r)$ determines the extrapolation length near the boundaries, a layer that is difficult to switch completely depending on how strong the anchoring is and on the applied voltage. The effect of this layer on the electrooptic response has been shown to be crucial in some cases [19].

The angle in the centre of the cell for the case of fixed boundary conditions (strong anchoring) can be approximated as follows [1]:

$$\theta_m \approx \theta_0 + \left(\frac{\pi}{2} - \theta_0\right)\sqrt{1 - 1/V_r^2}. \quad (20)$$

For the general case of finite anchoring (variable boundary conditions) the tilt angle in the middle of the cell can be calculated one time for each material and fitted with a power series. In our case we found the following series to describe its dependence on the voltage with accuracy better than 0.1°:

$$\theta_m \approx \theta_0 + \left(\frac{\pi}{2} - \theta_0\right)\sum_{n=0}^{15} a_n x^n, \quad (21)$$

where

$$x = b_2 - \frac{b_1 V_r^{\alpha}}{b_3 + b_1 V_r^{\alpha}},$$

so that it gives $\theta_m \approx \theta_0$ at zero voltage and $\theta_m \to 90^0$ as $V_r \to \infty$. For example, the coefficients found in the case of 5° pretilt angle and anchoring energy of 0.8 mJ m^{-2} are shown in Table 1. Figure 2 shows the good fit between the exact centre tilt angle (dashed curve) and that calculated based on Equation (21) and Table 1 (solid curve). The centre tilt angle for the infinite anchoring case is also plotted using Equation (20), showing the critical behaviour.

Note that the tilt angle at the centre of the cell is now a continuous function, i.e. the Frederick's transition is smoothed, contrary to the case of strong anchoring (fixed boundaries). Yet, we can define an

Table 1. The series coefficients for the tilt angle in the centre with an anchoring energy of 0.8 mJ m^{-2}.

Parameter	a_0	a_1	a_2	a_3	a_4	a_5	a_6	a_7	a_8	a_9
Value	1.0215	–1.4992	4.3732	–15.9523	14.5437	–1.6474	14.6940	–7.2271	–17.0105	–11.7976
Parameter	a_{10}	a_{11}	a_{12}	a_{13}	a_{14}	a_{15}	α	b_1	b_2	b_3
Value	21.7353	4.7309	–8.1260	–1.9599	14.6217	–10.4695	3.8760	1.0016	1.0143	1.2467

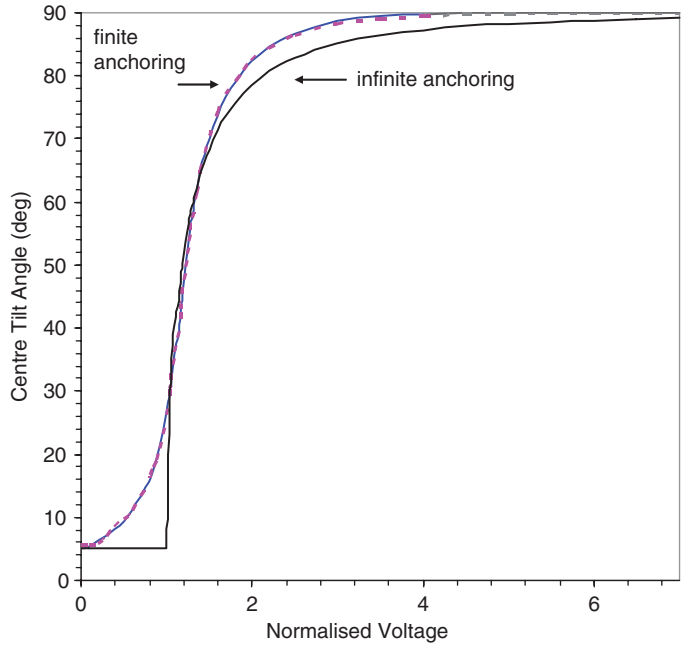

Figure 2. Dependence of the centre tilt angle on the normalised voltage for the case of finite anchoring $W = 0.8\,\mathrm{mJ\,m^{-2}}$ and pretilt angle $\theta_0 = 5^\circ$ with the calculation based on the exact simulation (solid blue curve) and the power expansion expression (dashed curve). The centre tilt angle calculated for the infinite anchoring case is shown as a solid black curve.

extrapolated threshold voltage V_{the}, which can be calculated numerically using the transcendental equation [20]:

$$\cot\left(\frac{\pi V_{\mathrm{the}}}{2V_{\mathrm{thf}}}\right) = \lambda_r \sqrt{\frac{K_{33}}{K_{11}}}\frac{V_{\mathrm{the}}}{V_{\mathrm{thf}}}. \qquad (22)$$

Depending on the anchoring strength, this equation shows that always $V_{\mathrm{the}} < V_{\mathrm{thf}}$ and they become equal for infinite anchoring. It also shows that the threshold has some dependence on the thickness.

5. Results and discussion

Figure 3 shows calculated tilt angle profiles for the case of fixed boundary orientations at different voltages both using the exact numerical approach described above and using the analytic expression given by Equation (19). The parameters of the LC material are similar to those of E44 of Merck: $\varepsilon_{||} = 22; \varepsilon_{\perp} = 5.2; K_{11} = 1.55 \times 10^{-11}\mathrm{N}; K_{33} = 2.8 \times 10^{-11}N; V_{\mathrm{thf}} = 1.0137\mathrm{V}$ and the parameter of the anchoring energy is $\xi = -0.22$. To achieve the fixed boundary conditions we used a very high anchoring energy $W = 2\,\mathrm{J\,m^{-2}}$. Note that the agreement is better than fractions of a degree for the entire range and the worst case is about 2° disagreement for the high-voltage case of $V_r = 6$ in a short region of tilt angles. As discussed before, the tilt angle profiles for the case of strong anchoring are universal in the sense that they neither depend on the thickness nor on the voltage, rather they depend on the normalised coordinate z_r and the normalised voltage V_r.

In Figure 4 the tilt profiles are presented for the case of finite anchoring energy $W = 1.8\,\mathrm{mJ\,m^{-2}}$ and pretilt angle $\theta_0 = 5^\circ$. The other parameters are the same as in Figure 1 except that now the thickness $d = 1.9$ mm should be mentioned because of the small dependence of λ_r on the thickness d as discussed earlier. The agreement is again as good as in the case of strong anchoring except that for the small voltage regime there is a 2° difference originating from disagreement between the values of the boundary tilt angle. In the small voltage regime V_r, Equation (16) might need a small correction, although we believe that for the design of LC devices this small discrepancy has a negligible effect on the simulated device output.

Figure 5 shows the tilt profile for smaller anchoring energy $W = 0.84\mathrm{mJm^{-2}}$ and pretilt angle $\theta_0 = 10^\circ$. The agreement in this case is similar to that in Figure 4, hence the conclusion is that the approximate analytic solution is satisfactory both for weak and strong anchoring as well as for large and small pretilt angles.

To conclude, approximate analytic expressions were presented for the steady-state tilt angle distribution in homogeneously aligned nematic LCs. The

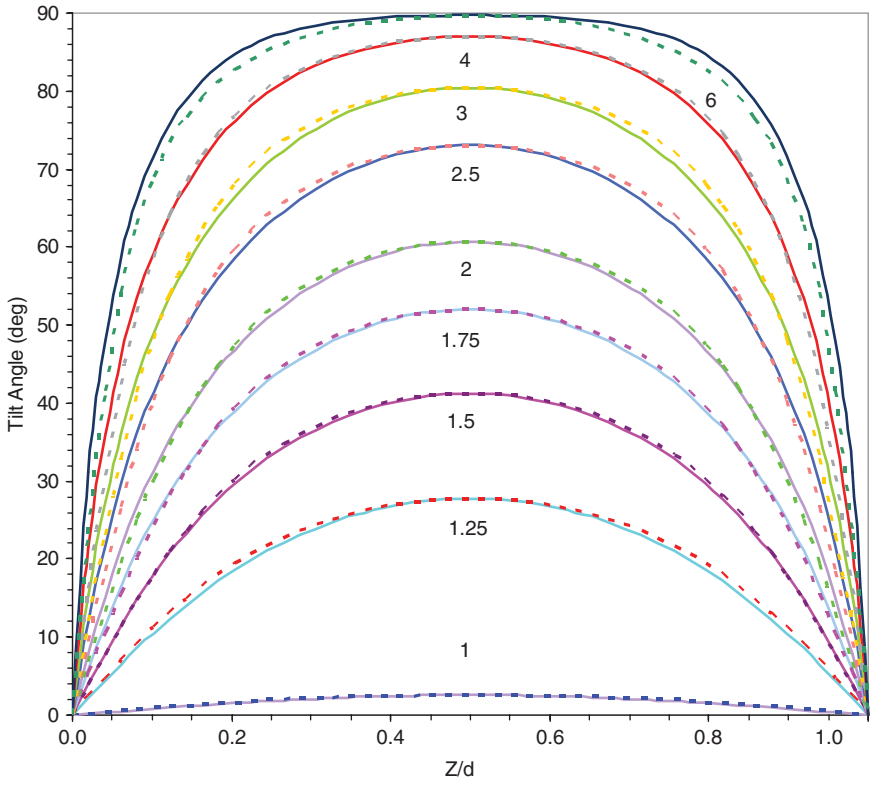

Figure 3. Tilt angle profiles for the case of strong anchoring $W = 2\,\mathrm{J\,m^{-2}}$ and pretilt angle $\theta_0 = 0.01^\circ$ at different normalised voltages as indicted calculated with the exact numerical approach (solid curve) and the analytic approach (dashed curve). The other parameters are given in the text.

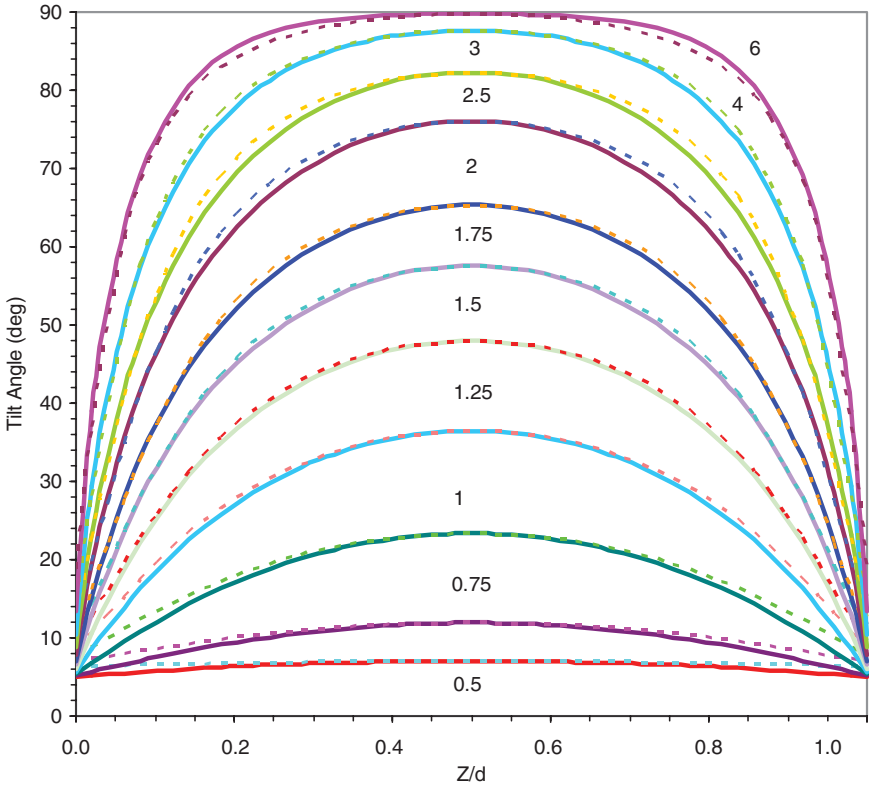

Figure 4. Tilt angle profiles for the case of finite anchoring $W = 1.8\,\mathrm{mJ\,m^{-2}}$ and pretilt angle $\theta_0 = 5^\circ$ at different normalised voltages as indicted calculated with the exact numerical approach (solid curve) and the analytic approach (dashed curve). The other parameters are as in Figure 3. The cell thickness is 1.9 μm.

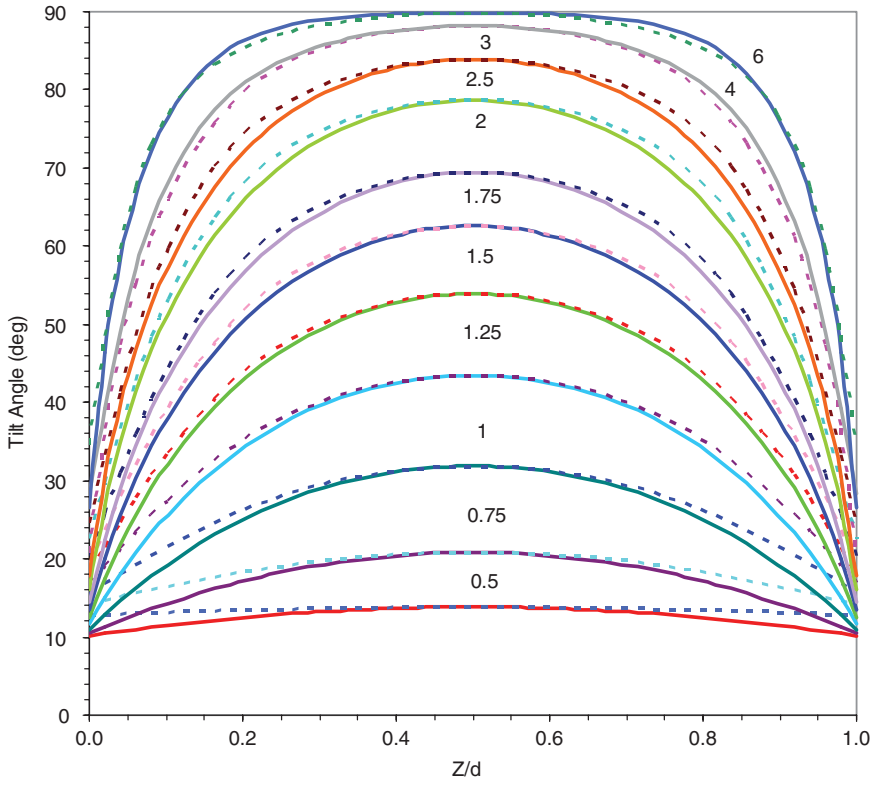

Figure 5. Tilt angle profiles for the case of small anchoring $W = 0.84\,\mathrm{mJ\,m^{-2}}$ and pretilt angle $\theta_0 = 10^{\circ}$ at different normalised voltages as indicted calculated with the exact numerical approach (solid curve) and the analytic approach (dashed curve). The other parameters are as in Figures 3 and 4.

agreement with the exact numerical solutions is excellent. These expressions are useful for easy design and understanding of the response of LC devices. It is believed that similar solutions can be found for other types of LCs, such as nematics in the hybrid geometry and ferroelectric LCs.

References

[1] Yang, D.-K.; Wu, S.-T. *Fundamental of Liquid Crystal Devices*; Wiley, 2006.
[2] Yokoyama, H. *Mol. Cryst. Liq. Cryst.* **1988**, *165*, 265–316.
[3] Jerome, B. *Rep. Prog. Phys.* **1991**, *54*, 391–451.
[4] Guochen, Y.; Jianru, S.; Ying, L. *Liq. Cryst.* **2000**, *27*, 875–882.
[5] Rapini, A.; Papoular, M. *J. Physique Coll.* **1969**, *30*, C4 54–56.
[6] Nehring, J.; Kmetz, A. R.; Scheffer, T.J. *J. Appl. Phys.* **1976**, *47*, 850–857.
[7] Welford, K.R.; Sambles, J.R. *Mol. Cryst. Liq. Cryst.* **1987**, *147*, 25–42.
[8] Yednak, C.A.R.; Igarashi, R.N.; Lenzi, E.K.; Evangelista, L.R. *Phys. Lett. A* **2006**, *358*, 31–36.
[9] Yang, K.H. *J. Physique* **1983**, *44*, 1051–1059.
[10] Barnik, M.I.; Blinov, L.M.; Korkishko, T.V.; Umansky, B.A.; Chigrinov, V.G. *Mol. Cryst. Liq. Cryst.* **1983**, *99*, 53–79.
[11] Subacius, D.; Pergamenshchik, V.M.; Lavrentovich, O.D. *Appl. Phys. Lett.* **1995**, *67*, 214–216.
[12] Seo, D.-S.; Kobayashi, S. *Appl. Phys. Lett.* **1995**, *66*, 1202–1204.
[13] Seo, D.-S.; Matsuda, H.; Oh-Ide, T.; Kobayashi, S. *Mol. Cryst. Liq. Cryst.* **1993**, *224*, 13–31.
[14] Andrienko, D.; Kurioz, Y.; Nishikawa, M.; Reznikov, Y.; West, J.L. *Jpn. J. Appl. Phys.* **2000**, *39*, 1217–1220.
[15] Deuling, H.J. *Mol. Cryst. Liq. Cryst.* **1972**, *19*, 123–131.
[16] Abdulhalim, I.; Moddel, G.; Clark, N.A. *Appl. Phys. Lett.* **1992**, *60*, 551–553.
[17] Maclennan, J.E.; Handschy, M.A.; Clark, N.A. *Liq. Cryst.* **1990**, *7*, 787–796.
[18] Stewart, I.W.; Momoniat, E. *Phys. Rev. E: Stat., Nonlinear, Soft Matter Phys.* **2004**, *69,* 061714-1–061714-9.
[19] Abdulhalim, I. *Europhys. Lett.* **1992**, *19,* 91–96; Erratum *Europhys. Lett.* **1992,** *19,* 439.
[20] Yang, K.H. *J. Appl. Phys.* **1983**, *54*, 6864–6867.